

The Possibility of Inflation in Asymptotically Safe Gravity

Sungwook E. Hong^{1,2*}, Young Jae Lee^{1†} and Heeseung Zoe^{1,3‡}

¹*Department of Physics, KAIST
Daejeon 305-701, Republic of Korea*

²*Department of Astronomy and Space Science,
Chungnam National University,
Daejeon 305-764, Republic of Korea*

³*Department of Physics,
Middle East Technical University,
06531, Ankara, Turkey*

May 2, 2019

Abstract

We examine the inflationary modes in the cubic curvature theories in the context of asymptotically safe gravity. On the phase space of the Hubble parameter, there exists a critical point which corresponds to the slow-roll inflation in Einstein frame. Most of the e-foldings are attained around the critical point for each inflationary trajectories. If the coupling constants g_i have the parametric relations generated as the power of the relative energy scale of inflation H_0 to the ultraviolet cutoff Λ , a successful inflation with more than 60 e-foldings occurs near the critical point. When the inflation energy scale is comparable to the cutoff, the quantum fluctuation could exit the inflationary phase with insufficient e-foldings.

1 Introduction

As is well-known, in four dimensional gravity, conventional wisdom gained in field theory does not work in reconciling unitary and renormalizability. In particular, the unitarity of the non-renormalizable Einstein-Hilbert theory is ruined by the presence of a massive ghost when quadratic terms in the curvature—that make the theory renormalizable—are added [1]. This bleak state of affairs might change if Weinberg’s long-standing conjecture of “asymptotic safety” works [2]. Leaving the details for an excellent review [3] and the references therein, let us note that asymptotic safety of gravity relies on the assumption that a non-gaussian fixed point exists for a finite gravity theory with infinitely many coupling constants and that the critical surface is finite dimensional, upgrading the theory to be a predictive one. Recently, there has been a revival of interest in asymptotically safe gravity and are some encouraging results showing the possible existence of an asymptotically safe gravity [4].

*eostm@muon.kaist.ac.kr

†noasac@muon.kaist.ac.kr

‡heezoe@gmail.com

More recently, inflationary scenarios based on the asymptotically safe gravity are suggested [5] [6]. The generic form of their action is

$$S = \int d^4x \sqrt{-g} \sum_{l,m,n} \Lambda^{4-(2l+4m+4n)} c_{lmn} R^l (R^2_{\mu\nu})^m (R^2_{\mu\nu\rho\sigma})^n, \quad (1)$$

where Λ is the ultraviolet cutoff scale of the theory and c_{lmn} are dimensionless coupling constants. Weinberg showed that, without introducing a scalar field, there exist de Sitter solutions and the modes of the Hubble parameter which can exit out of the pure de Sitter phase [5].

In order to promote the inflationary phase without a scalar field, some higher derivative terms should be crucial in the very early universe in order to give enough e-foldings. Since our current universe has almost pure Einstein's gravity, however, these higher derivative terms must become negligible somehow at the present era. Hence, there must be a nontrivial mechanism which controls the evolution of c_{lmn} ¹ and it will produce observable signatures such as the production of primordial gravitational wave and the density perturbation for the structure formation, as in dilaton string cosmology [7].

In this paper, building in Weinberg's work [5], we study the phase space of the Hubble parameter, (H, \dot{H}) determined by the classical equations derived from the variation of the action. In the phase space, a proper trajectory for successful inflation should go to the non-inflationary era after giving more than 60 e-foldings. We will see that the existence of such a trajectory depends on the algebraic equation, $\mathcal{C}(H) = 0$ whose solutions decide the critical points where slow-roll inflation is possible. It gives non-trivial conditions for the coupling constants and the relative energy scale of inflation to the cutoff.

However, since the quantum fluctuations of the inflaton field can hugely affect its classical dynamics in the standard slow-roll inflation, we should be careful about whether the quantum effects on the Hubble parameter may alter the e-foldings calculated along the classical trajectories. There is no simple way to estimate the quantum effects on the Hubble parameter for generic higher derivative theories. So we will estimate them only in the context of $f(R)$ gravity where we can change the given action to Einstein's gravity plus a scalar field. We will calculate the quantum fluctuations of the scalar field and then convert them into the random walks on the Hubble parameter along the classical trajectory.

This paper is organized as follows. In Section 2, we consider conditions for successful inflation with enough e-foldings in the R^2 - and R^3 - gravities using their conformally related partners. In Section 3, we consider the classical inflationary trajectories by analyzing the phase space of the Hubble parameter. In Section 4, we consider the quantum fluctuations and examine how they affect the e-foldings. We discuss possible future works in Section 5.

2 Conditions for slow-roll inflation

Before going into the general cases, we first discuss the possibility of inflation from a cubic curvature theory based on the Ricci scalar alone,²

$$S = - \int d^4x \sqrt{-g} [\Lambda^4 g_0 + \Lambda^2 g_1 R + g_2 R^2 + \Lambda^{-2} g_3 R^3]. \quad (2)$$

¹Some previous works, e.g. [8], assumed c_{lmn} as constants.

²We follow Weinberg's signature convention of the metric, $(+, -, -, -)$ and the Riemann tensor $R^\mu_{\nu\alpha\beta} = +\partial_\alpha\Gamma^\mu_{\nu\beta} + \dots$.

We can investigate the possibility of inflation by directly tracing the Hubble parameter and find conditions on g_i 's that will produce enough e-foldings. Also, we can rewrite this action as Einstein's gravity plus a scalar field by conformally rescaling the metric and discuss inflationary conditions. So let us compare these two results to gain an understanding of how to deal with general higher derivative gravities. In this section, the main goal will be to understand rather crudely the conditions on g_i 's which yield enough e-foldings, namely, we will explore parametric relations between g_i 's. In the following sections, accurate numerical simulations between g_i 's will be given.

2.1 Classical analysis with the Hubble modes

Now we will find the inflationary trajectories by directly analyzing the equations of motion coming from the variation of (2) as Weinberg did in [5]. We will check whether it allows a de Sitter solution and then look for the constraints on g_i 's by requiring enough e-foldings.

The physical degrees of freedom around FRW background, $ds^2 = dt^2 - a(t)^2 d\vec{x}^2$, are encoded in a single equation of the Hubble parameter, $H(t) = \dot{a}/a$, which comes from the variation of the action [5, 9],

$$\begin{aligned} \mathcal{N}(t) &\equiv -\frac{2}{\Lambda^4} \left(\frac{\delta S}{\delta g_{00}} \right)_{\text{FRW}} & (3) \\ &= -g_0 + g_1 \Lambda^{-2} (6H^2) - g_2 \Lambda^{-4} (216H^2 \dot{H} - 36\dot{H}^2 + 72H\ddot{H}) \\ &\quad + g_3 \Lambda^{-6} \left[-864H^6 + 7776H^4 \dot{H} + 3240H^2 \dot{H}^2 - 432\dot{H}^3 + 216H\ddot{H}(12H^2 + 6\dot{H}) \right] \\ &= 0. \end{aligned}$$

The dimensionless quantity, H/Λ , characterizes the energy scale of inflation to the cutoff scale. This quantity is expected to be small, e.g. of the order of 10^{-5} in [9], so that it would be helpful to collect the terms of (3) accordingly, to analyze the behavior of the Hubble parameter.

2.1.1 $g_3 \lesssim g_1$

We start considering a purely de Sitter solution by taking $H(t) = H_0$, and then (3) yields

$$-g_0 + 6g_1 \left(\frac{H_0}{\Lambda} \right)^2 - 864g_3 \left(\frac{H_0}{\Lambda} \right)^6 = 0. \quad (4)$$

Since the third term is expected to be small, we can find a simple solution,

$$H_0^2 = \frac{g_0}{6g_1} \Lambda^2, \quad (5)$$

which relates g_0 and g_1 as

$$g_0 \sim g_1 \left(\frac{H_0}{\Lambda} \right)^2. \quad (6)$$

Now we investigate the classical behavior around the de Sitter solution in the linear approximation by putting a time dependent mode,

$$H(t) = H_0 + \delta(t). \quad (7)$$

If $\delta(t) \propto \exp(\xi H_0 t)$ and $\xi > 0$, then its e-folding number is $N_{\text{efold}} \sim 1/\xi$ [5]. By considering the lowest order terms in H_0/Λ and $\delta(t)$ from (3), one obtains

$$12 \frac{g_1}{\Lambda^2} \delta(t) - 216 \frac{g_2}{\Lambda^4} H_0 \dot{\delta}(t) = 0, \quad (8)$$

whose solution is

$$\delta(t) \propto \exp \left[\frac{g_1}{18g_2} \left(\frac{\Lambda}{H_0} \right)^2 H_0 t \right]. \quad (9)$$

A discussion of the signature of the coupling constants is in order. Attractive gravity requires $g_1 > 0$ and unitarity of the theory at the linearized level requires $g_2 > 0$ for de Sitter and flat background³. The requirement that one has more than 60 e-foldings,

$$N_{\text{efold}} = \frac{18g_2}{g_1} \left(\frac{H_0}{\Lambda} \right)^2 \gtrsim 60 \quad (10)$$

leads to

$$g_1 \sim g_2 \left(\frac{H_0}{\Lambda} \right)^2, \quad (11)$$

which is a similar relation as (6).

2.1.2 $g_3 \gg g_1$

We have seen that g_3 term could not contribute to the construction of de Sitter phase. However, if g_3 is large enough to compensate the suppression of $(H_0/\Lambda)^4$, then the cubic terms would be important. From (4), we can read off the magnitude of g_3 for such a realization,

$$g_3 \sim g_1 \left(\frac{\Lambda}{H_0} \right)^4. \quad (12)$$

Then by considering higher order terms in H_0/Λ and $\delta(t)$ from (3), one has

$$\begin{aligned} -5184 \frac{g_3}{\Lambda^6} H_0^5 \delta(t) + 12 \frac{g_1}{\Lambda^2} H_0 \delta(t) + 7776 \frac{g_3}{\Lambda^6} H_0^4 \dot{\delta}(t) - 216 \frac{g_2}{\Lambda^4} H_0^2 \dot{\delta}(t) \\ + 2592 \frac{g_3}{\Lambda^6} H_0^3 \ddot{\delta}(t) - 72 \frac{g_2}{\Lambda^4} H_0 \ddot{\delta}(t) = 0. \end{aligned} \quad (13)$$

If we assume that $\delta(t)$ can give enough e-foldings, then we may put $\delta(t) \propto \exp(H_0/60t)$ and (13) gives a solution for g_3 in terms of g_1 and g_2 ,

$$g_3 = \frac{50}{21057} g_1 \left(\frac{\Lambda}{H_0} \right)^4 - \frac{181}{252684} g_2 \left(\frac{\Lambda}{H_0} \right)^2, \quad (14)$$

which implies

$$g_3 \sim 10^{-2\sim 3} \times g_1 \left(\frac{\Lambda}{H_0} \right)^4 \sim 10^{-2\sim 3} \times g_2 \left(\frac{\Lambda}{H_0} \right)^2, \quad (15)$$

and g_3 may be negative.

We have explored the relations between the coupling constants, g_i , in a toy model of $f(R)$ gravity up to the cubic order. If we rescale g_i in compact forms,

$$\bar{g}_0 \equiv g_0 \left(\frac{\Lambda}{H_0} \right)^6, \quad \bar{g}_1 \equiv g_1 \left(\frac{\Lambda}{H_0} \right)^4, \quad \bar{g}_2 \equiv g_2 \left(\frac{\Lambda}{H_0} \right)^2, \quad (16)$$

then the condition for successful inflation with more than 60 e-foldings is

$$\bar{g}_0 \sim \bar{g}_1 \sim \bar{g}_2, \quad \text{and} \quad g_3 \lesssim 10^{-2\sim 3} \times \bar{g}_2. \quad (17)$$

It is quite a crude estimation but provides a sound ground for numerical simulations.

³Without referring to the unitarity issues, we might require $g_2 > 0$ just to have an exit from de Sitter phase.

2.2 Conformally related Einstein action

It is well known that $f(R)$ gravity can be mapped to Einstein's gravity plus a scalar field after the metric is conformally scaled ($g_{\mu\nu} \rightarrow \Omega^2 g_{\mu\nu}$). Here, we will conformally transform (2) into the Einstein action, and check its slow-roll inflationary condition. (2) can be expressed as

$$S = -\Lambda^2 g_1 \int d^4x \sqrt{-g} f(R), \quad (18)$$

where

$$f(R) \equiv G_0 + G_1 R + G_2 R^2 + G_3 R^3, \quad (19)$$

and

$$G_0 \equiv \Lambda^2 \frac{g_0}{g_1}, \quad G_1 \equiv 1, \quad G_2 \equiv \Lambda^{-2} \frac{g_2}{g_1}, \quad G_3 \equiv \Lambda^{-4} \frac{g_3}{g_1}. \quad (20)$$

We assume g_i 's might have renormalization group flows and inflation would occur at a certain high energy scale. It means that Planck mass \tilde{M}_p can be different from 10^{19} GeV of our present low energy universe. We have

$$\Lambda^2 g_1 = \frac{1}{16\pi\tilde{G}} = \frac{\tilde{M}_p^2}{2}. \quad (21)$$

According to (7.7) and (7.10) in [10], the scalar field and its potential are given by

$$\phi = \frac{\sqrt{6}\tilde{M}_p}{2} \ln \frac{\partial f}{\partial R} = \sqrt{3\Lambda^2 g_1} \ln(G_1 + 2G_2 R + 3G_3 R^2), \quad (22)$$

and

$$V(\phi) = \frac{\tilde{M}_p^2}{2} \frac{f(R) - R\partial f/\partial R}{(\partial f/\partial R)^2} = \Lambda^2 g_1 \frac{G_0 - G_2 R^2 - 2G_3 R^3}{(G_1 + 2G_2 R + 3G_3 R^2)^2}. \quad (23)$$

Applying the slow-roll approximation, the equations of motion for the scalar field are

$$3H_E \dot{\phi} = -\frac{\partial V}{\partial \phi} \quad \text{and} \quad H_E^2 = \frac{1}{3\tilde{M}_p^2} V(\phi), \quad (24)$$

where the slow-roll parameters satisfy

$$\epsilon \equiv \frac{\tilde{M}_p^2}{2} \left(\frac{\partial V/\partial \phi}{V} \right)^2 \ll 1 \quad \text{and} \quad \eta \equiv \tilde{M}_p^2 \left(\frac{\partial^2 V/\partial \phi^2}{V} \right) \ll 1. \quad (25)$$

Let's assume that the slow-roll conditions are satisfied near a certain ϕ_0 (and the corresponding R_0). Then from $\epsilon \ll 1$, one has

$$\epsilon(\phi_0) = 3 \left(\frac{2G_0 + G_1 R_0 - G_3 R_0^3}{G_0 - G_2 R_0^2 - 2G_3 R_0^3} \right)^2 \ll 1, \quad (26)$$

which is sufficiently satisfied if one sets

$$2G_0 + G_1 R_0 - G_3 R_0^3 \approx 0, \quad (27)$$

and the denominator should not vanish. And from $\eta \ll 1$,

$$\begin{aligned} \eta(\phi_0) &= \frac{(8G_0 G_2 - G_1^2) + (24G_0 G_3 + 2G_1 G_2)R_0 + 12G_1 G_3 R_0^2 + 2G_2 G_3 R_0^3 - 3G_3^2 R_0^4}{3(G_2 + 3G_3 R_0)(G_0 - G_2 R_0^2 - 2G_3 R_0^3)} \\ &\ll 1, \end{aligned} \quad (28)$$

which is sufficiently satisfied if one sets

$$(8G_0G_2 - G_1^2) + (24G_0G_3 + 2G_1G_2)R_0 + 12G_1G_3R_0^2 + 2G_2G_3R_0^3 - 3G_3^2R_0^4 \approx 0, \quad (29)$$

and the denominator should not vanish.

Now, if we assume that $g_3 \approx 0$, then (27) and (29) give

$$R_0 = -\frac{2G_0}{G_1} \quad \text{and} \quad G_1^2 = 6G_0G_2, \quad (30)$$

which implies

$$g_1^2 \sim g_0g_2. \quad (31)$$

In this case, the slow-roll conditions are satisfied if

$$g_0 \sim g_1 \left(\frac{H_0}{\Lambda} \right)^2 \quad \text{and} \quad g_1 \sim g_2 \left(\frac{H_0}{\Lambda} \right)^2. \quad (32)$$

And if $g_3 \gtrsim 0$, (27) and (29) give

$$(G_1 - 3G_3R_0^2)(G_1 + 2G_2R_0 + 3G_3R_0^2) \approx 0. \quad (33)$$

Since $G_1 + 2G_2R_0 + 3G_3R_0^2$ cannot be zero by (22), $G_1 - 3G_3R_0^2 \approx 0$. Then, from (27),

$$R_0 = -\frac{3G_0}{G_1} \quad \text{and} \quad G_3 = \frac{G_1^3}{27G_0^2}, \quad (34)$$

and its Hubble parameter satisfies

$$H_0^2 = \frac{1}{6} \frac{G_0 - G_2R_0^2 - 2G_3R_0^2}{(G_1 + 2G_2R_0 + 3G_3R_0^2)^2} = \frac{1}{8} \frac{G_0}{G_1^2 - 3G_0G_2} = \frac{\Lambda^2}{8} \frac{g_0g_1}{g_1^2 - 3g_0g_2}. \quad (35)$$

This implies necessarily both g_1^2 and $3g_0g_2$ are in the same order as $g_0g_1(\Lambda/H_0)^2$; that is,

$$g_0 \sim g_1 \left(\frac{H_0}{\Lambda} \right)^2 \quad \text{and} \quad g_1 \sim g_2 \left(\frac{H_0}{\Lambda} \right)^2, \quad (36)$$

and from (34),

$$g_2 \sim 10^{-2} \times g_3 \left(\frac{H_0}{\Lambda} \right)^2. \quad (37)$$

These conditions are equivalent to what we found before. Then we may claim that (17) can necessarily satisfy the slow-roll conditions in the context of a scalar field plus Einstein's gravity. Note that this exercise of mapping the $f(R)$ action to Einstein's gravity plus a scalar field was necessary to see the slow-roll conditions that are well-defined for the scalar field. Namely, in the pure higher derivative gravity, the slow-roll conditions were not transparent.

3 Analysis on the phase space of the Hubble parameter

In the previous section, we considered the $f(R)$ gravity case and found the conditions on g_i 's which give enough e-foldings. Now we numerically study the classical inflationary trajectories and their e-foldings in the phase diagrams (H, \dot{H}) generated by the nonlinear equation of motion.

We will see that g_i 's affect the classical trajectories of the phase space and decide cosmological viability. The trajectories in the phase space should satisfy the following conditions for successful inflation:

1. The inflationary phase should be stopped leading to the standard post-inflationary history. A proper trajectory should go into the non-inflationary era, $\ddot{a} < 0$.
2. There must exist the attractor behavior for the naturalness of inflation. There should be some region in the phase diagram where all nearby trajectories converges to the non-inflationary era.
3. A proper trajectory should give e-foldings more than 60 while moving to the non-inflationary era.

3.1 $f(R)$ gravity

The governing equation (3), which was derived from $f(R)$ gravity action (2), can be rewritten with the redefinition of the Hubble parameter and its derivatives as

$$\begin{aligned}
\bar{\mathcal{N}}(h, h', h'') &\equiv -\frac{2\Lambda^2}{H_0^6} \left(\frac{\delta S}{\delta g_{00}} \right)_{\text{FRW}} = 0 \\
&= (-\bar{g}_0 + 6\bar{g}_1 h^2 - 864g_3 h^6) + (-216\bar{g}_2 h^2 + 7776g_3 h^4) h' \\
&\quad + (36\bar{g}_2 + 3240g_3 h^2) h'^2 - 432g_3 h'^3 \\
&\quad + [(-72\bar{g}_2 h + 2592g_3 h^3) + 1296g_3 h h'] h'',
\end{aligned} \tag{38}$$

where $h \equiv H/H_0$, $h' \equiv dh/d(H_0 t)$, and $h'' \equiv d^2 h/d(H_0 t)^2$.

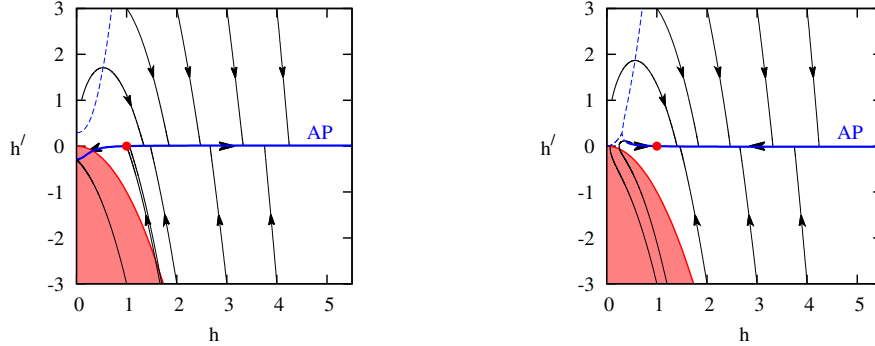


Figure 1: The general behavior of the classical trajectories in (h, h') phase diagram with $g_3 = 0$. Left: $(\bar{g}_0, \bar{g}_1, \bar{g}_2, g_3) = (3, 0.5, 1, 0)$. Right: $(\bar{g}_0, \bar{g}_1, \bar{g}_2, g_3) = (3, 0.5, -1, 0)$. Red area: $\ddot{a} < 0$, the non-inflationary era. Red dot: h_* -point around which inflation is maximized, that is $h = 1$ and $h' = h'' = 0$. Blue dash: $h'' = 0$. Blue solid: the asymptotic path(AP), that is $h'' = 0$, on which there exists the h_* -point. In Left, the e-foldings, N_{efold} around the h_* -point is numerically estimated to be 200.

Figure 1 (Left) shows the general behavior of the classical trajectories in (h, h') phase diagram with $g_3 = 0$. There exists an asymptotic path(AP) with $h'' = 0$, where all classical trajectories converge to either $h = 0$ or $h = \infty$. The de Sitter phase is at $(h, h') = (1, 0)$, represented by a red dot in the figure. A proper trajectory for successful inflation should pass through this dS point and end up with non-inflationary era, represented by the red area.

Since the AP satisfies $h'' = 0$ from (38), along it, one must have

$$\begin{aligned}
\mathcal{B}(h, h') &\equiv -\bar{\mathcal{N}}(h, h', 0) = 0 \\
&= 432g_3 h'^3 - (3240g_3 h^2 + 36\bar{g}_2) h'^2 - (7776g_3 h^4 - 216\bar{g}_2 h^2) h' \\
&\quad + (864g_3 h^6 - 6\bar{g}_1 h^2 + \bar{g}_0) = 0.
\end{aligned} \tag{39}$$

Like a slow-roll point in inflationary model, there may exist a point in the phase diagram that tends to keep its current state forever. This is possible at certain points, $h = h_*$ where both h' and h'' are zero, that is,

$$\mathcal{C}(h_*) \equiv \mathcal{B}(h_*, 0) = 864g_3h_*^6 - 6\bar{g}_1h_*^2 + \bar{g}_0 = 0. \quad (40)$$

We call these points, i.e. the roots of (40), h_* -points. Actually, (40) is a different expression of (4). If (4) has a de Sitter solution, then (40) would have $h_* = 1$ as a root and the trajectories around this point in the phase diagram would be crucial for a successful inflation.

In Figure 1 (Left), h_* -point acts as an attractor along the normal direction to the AP and as a repeller along it. If a trajectory approaches the AP at a point $h > h_*$ then it will follow the AP which goes far away from the non-inflationary region ($\ddot{a} < 0$) and the inflation never ends, which does not fit to our universe. On the other hand, if a trajectory approaches the AP at a point $h \ll h_*$, then it will soon fall into the non-inflationary region without generating enough e-foldings, which also does not fit to our universe. Therefore, in order to explain our universe the classical trajectory needs to approach the AP at the point where h is equal to, or slightly smaller than h_* .

However, $g_2 < 0$ severely changes the asymptotic behavior so that h_* -point is an attractor from all directions in Figure 1 (Right). In this case, if a trajectory approaches the h_* -point, then it would stay there forever and the inflationary phase cannot be stopped, which does not fit to our universe again.

We can easily see that for $g_3 = 0$, the sign of g_2 changes the asymptotic behavior around the h_* -point. Around the h_* -point where $h = 1$, since $h'^2 \ll h'$ and $h'' = 0$ in (38), one has

$$\bar{\mathcal{N}}(h, h', 0) \approx -\bar{g}_0 + 6\bar{g}_1h^2 - 216\bar{g}_2h^2h' \approx 0, \quad (41)$$

which gives

$$h' \approx \frac{1}{g_2} \left(\frac{\bar{g}_1}{36} - \frac{\bar{g}_0}{216h^2} \right) = \frac{\bar{g}_1}{36\bar{g}_2h^2} (h^2 - 1), \quad (42)$$

from the fact that at $h = 1$, one has $h' = 0$, which implies $\bar{g}_0 = 6\bar{g}_1$. Now one can see that for $g_2 > 0$, h' is a monotonically increasing function of h around the h_* -point from (42). For $h < 1$, one has $h' < 0$ but for $h > 1$, $h' > 0$. However, for $g_2 < 0$, h' is a monotonically decreasing function of h so that for $h < 1$ one has $h' > 0$ but for $h > 1$, $h' < 0$. This explains completely the asymptotic behavior around the h_* -points in Figure 1. Actually, $g_2 < 0$ is ruled out by the requirement of unitarity of the free theory, as we mentioned earlier, but now we check it is also not allowed in the context of inflationary cosmology.

3.1.1 How to get an inflationary trajectory

The fact that $h_* = 1$ is a solution of (40) would give tight constraints on g_i 's and be useful to predict the behavior along the AP of the phase diagram. Putting $h_* = 1$ in (40) yields,

$$g_3 = \frac{1}{864} (6\bar{g}_1 - \bar{g}_0). \quad (43)$$

Let us note that we had four parameters (g_0, g_1, g_2, g_3) in (4) to fix H_0 by solving (4). However, we have changed our parameter set to $(\bar{g}_0, \bar{g}_1, \bar{g}_2, H_0)$ as (40) and can fix g_3 by requiring $h_* = 1$.

Figure 2 shows that there is no possible inflationary trajectory with enough e-foldings when g_i 's do not satisfy (43). In this case, no h_* -point exists or even if it does exist, it is too close to the non-inflationary era to give enough e-foldings.

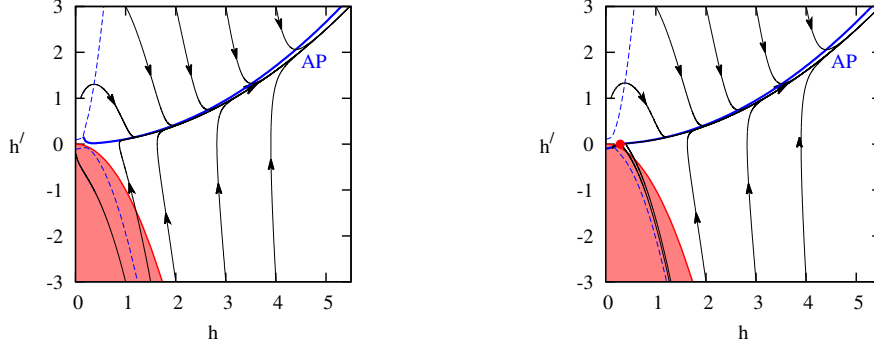


Figure 2: The general behavior of the classical trajectories in (h, h') phase diagram when g_i 's do not satisfy (43). Left: $(\bar{g}_0, \bar{g}_1, \bar{g}_2, g_3) = (1, 1, 1, 1)$. Right: $(\bar{g}_0, \bar{g}_1, \bar{g}_2, g_3) = (1, 1, 1, -1)$. The asymptotic path(AP)s, blue solid lines, are the curves going to the top-right corner. In Left, the h_* -point does not exist. In Right, h_* -point is at $h < 1$. In both cases, $N_{\text{efold}} \ll 10$.

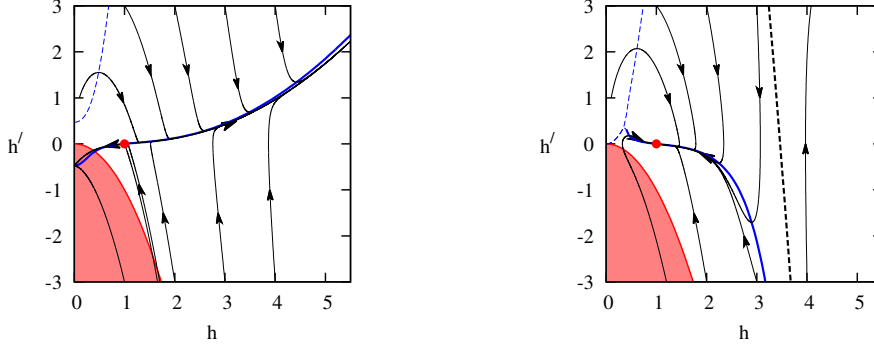


Figure 3: The general behavior of the classical trajectories in (h, h') phase diagram with $g_3 < 0$. Left: $(\bar{g}_0, \bar{g}_1, \bar{g}_2, g_3) = (8, 1, 1, -1/432)$ with $N_{\text{efold}} = 90$. Right: $(\bar{g}_0, \bar{g}_1, \bar{g}_2, g_3) = (8, 1, -1, -1/432)$. The directions of trajectories around the divergence curve(black dash) given by (45) are opposite and the h_* -point is under it. In Left, the divergence curve is too under the h_* -point so that it is not shown in the figure and it does not affect the direction of trajectories near the h_* -point. In Right, the divergence curve blows up and the direction of trajectories near the h_* -point is opposite to Left.

By using (43), it is possible to simplify (40) to see the roots clearly as follows,

$$\mathcal{C}(h_*) = (h_*^2 - 1) \left(h_*^2 + \frac{1}{2} + \frac{1}{2} \sqrt{1 + \frac{4\bar{g}_0}{6\bar{g}_1 - \bar{g}_0}} \right) \left(h_*^2 + \frac{1}{2} - \frac{1}{2} \sqrt{1 + \frac{4\bar{g}_0}{6\bar{g}_1 - \bar{g}_0}} \right) = 0. \quad (44)$$

When $g_3 < 0$, i.e. $\bar{g}_0 < 6\bar{g}_1$, still there is only one (real) solution, $h_* = 1$, since $\sqrt{1 + \frac{4\bar{g}_0}{6\bar{g}_1 - \bar{g}_0}}$ must be imaginary. Figure 3 (Left) shows that we can find a proper inflationary trajectory around $h_* = 1$ with $g_2 > 0$. On the other hand, for $g_2 < 0$, the direction of the trajectory is opposite when one crosses the line at which h'' diverges, represented by the black dash in Figure 3 (Right). As h'' is divergent, the terms multiplying h'' of (38) become important. On this divergence curve, these terms should vanish,

$$(-72\bar{g}_2 h + 2592g_3 h^3) + 1296g_3 h h' = 0 \quad \rightarrow \quad h' = -2h^2 + \frac{\bar{g}_2}{18g_3}. \quad (45)$$

The direction of the trajectory at very large h is outward, e.g. both h and h' increase, but since the divergence curve is *over* $h_* = 1$, the direction of the trajectory at $h \gtrsim 1$

is inward, e.g. h decreases, and also the direction at $h \lesssim 1$ is outward. In the case $g_2 < 0$, therefore, $h_* = 1$ is an attractor so that all nearby trajectories cannot go to the non-inflationary region.

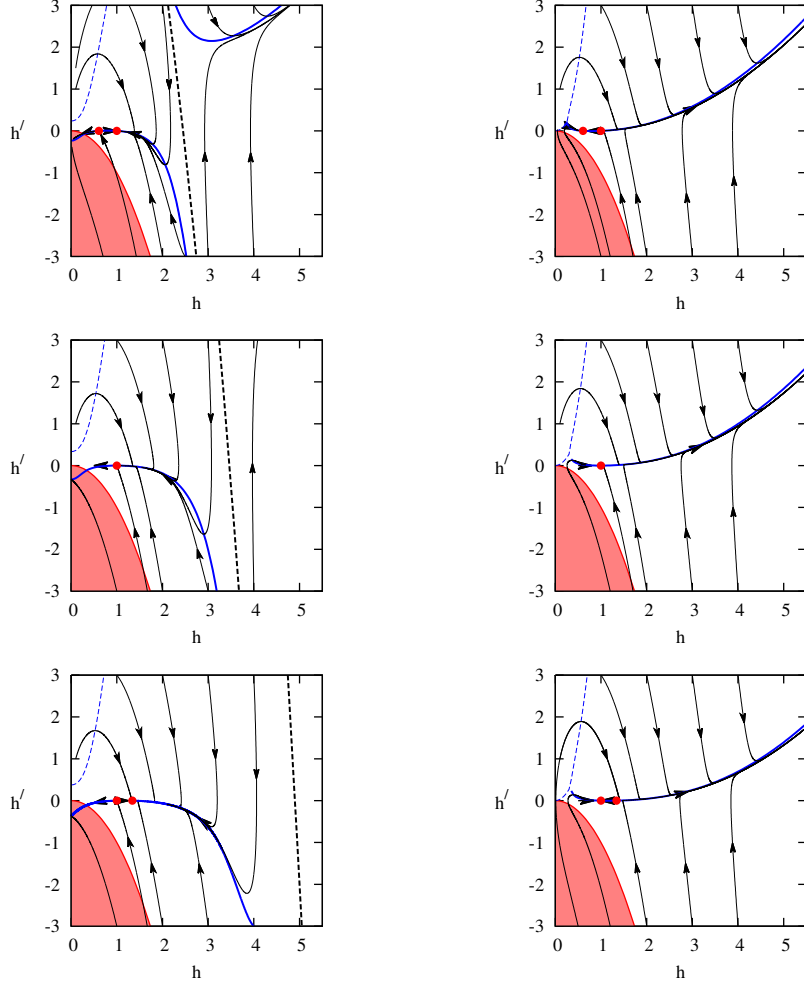


Figure 4: The general behavior of the classical trajectories in (h, h') phase diagram with $g_3 > 0$. Top: two roots with $h_{1*} = 1$ and $h_{2*} < 1$: left: $(\bar{g}_0, \bar{g}_1, \bar{g}_2, g_3) = (2, 1, 1, 1/216)$ and $N_{\text{efold}} = 60$; right: $(\bar{g}_0, \bar{g}_1, \bar{g}_2, g_3) = (2, 1, -1, 1/216)$. Middle: one with $h_* = 1$: left: $(\bar{g}_0, \bar{g}_1, \bar{g}_2, g_3) = (4, 1, 1, 1/432)$ and $N_{\text{efold}} = 100$; right: $(\bar{g}_0, \bar{g}_1, \bar{g}_2, g_3) = (4, 1, -1, 1/432)$. Bottom: two roots with $h_{1*} = 1$ and $h_{2*} > 1$: left: $(\bar{g}_0, \bar{g}_1, \bar{g}_2, g_3) = (5, 1, 1, 1/864)$ and $N_{\text{efold}} = 200$; right: $(\bar{g}_0, \bar{g}_1, \bar{g}_2, g_3) = (5, 1, -1, 1/864)$. Red dot: the h_* -point. Red area: the non-inflationary era. Blue solid: the asymptotic path(AP) where $h'' = 0$. Blue dash: $h'' = 0$. Black dash: the divergence curve where h'' diverges.

When $g_3 > 0$, i.e. $\bar{g}_0 > 6\bar{g}_1$, we have more possibilities. From (44), there would be two real and positive roots,

$$h_{1*} = 1, \quad \text{or} \quad h = h_{2*} \equiv \sqrt{-\frac{1}{2} + \frac{1}{2}\sqrt{1 + \frac{4\bar{g}_0}{6\bar{g}_1 - \bar{g}_0}}}. \quad (46)$$

By straightforward calculations, one observes that there are three distinct cases,

- $\bar{g}_0 > 4\bar{g}_1$: $h_{1*} = 1$ and $h_{2*} > 1$.

If $g_2 > 0$, then from (45) the divergence curve is *over* h_* 's, and $h_{2*} > 1$ is an attractor and $h_{1*} = 1$ is a repeller. Therefore, we can find a proper inflationary trajectory around $h_{1*} = 1$ (Top-left of Figure 4).

On the other hand, if $g_2 < 0$, then the divergence curve is *under* h_* 's, now $h_{2*} > 1$ is a repeller and $h_{1*} = 1$ is an attractor, and there is no proper inflationary trajectory (Top-right of Figure 4).

- $\bar{g}_0 = 4\bar{g}_1$: $h_{1*} = h_{2*} = 1$.

In this case, if $g_2 > 0$, then $h_* = 1$ is an attractor in the direction $h > h_*$ and a repeller in the direction $h < h_*$, so we can find a proper inflationary trajectory around $h_* = 1$ (Middle-left of Figure 4).

On the other hand, if $g_2 < 0$, then $h_* = 1$ is a repeller in the direction $h > h_*$ and an attractor in the direction $h < h_*$, so there is no proper inflationary trajectory (Middle-right of Figure 4).

- $\bar{g}_0 < 4\bar{g}_1$: $h_{1*} = 1$ and $h_{2*} < 1$. This is the same as the case $\bar{g}_0 > 4\bar{g}_1$, except that we can find a proper inflationary trajectory around $h_{2*} < 1$ (Bottom of Figure 4).

3.1.2 e-foldings

Assuming that there exists a trajectory passing near the h_* -point, its e-foldings will come mainly from the region near the point. Since after the trajectory passes the h_* -point as it follows the AP, its position $(h_* + \Delta h, \Delta h')$ satisfies

$$\Delta h' = \frac{432g_3h_*^4 - \bar{g}_1}{18h_*(36g_3h_*^2 - \bar{g}_2)} \Delta h, \quad (47)$$

which follows from (38). Therefore, the time scale to enter and escape the h_* -point is

$$\Delta t \sim 2 \frac{1}{H_0} \frac{\Delta h}{\Delta h'} = \frac{1}{H_0} \frac{36h_*(36g_3h_*^2 - \bar{g}_2)}{432g_3h_*^4 - \bar{g}_1}, \quad (48)$$

and the e-foldings generated near the h_* -point are

$$\Delta N_{\text{efold}}^* \sim H(h_*) \Delta t = \frac{36h_*^2(36g_3h_*^2 - \bar{g}_2)}{432g_3h_*^4 - \bar{g}_1} \gtrsim 60. \quad (49)$$

If $g_3 = 0$, then $h_* = 1$ and (49) becomes

$$36 \frac{\bar{g}_2}{\bar{g}_1} \gtrsim 60 \quad \rightarrow \quad \frac{\bar{g}_2}{\bar{g}_1} \gtrsim \frac{5}{3}, \quad (50)$$

which is essentially the same result as (10).

If $g_3 \neq 0$, then (49) becomes

$$\frac{36h_*^2(36g_3h_*^2 - \bar{g}_2)}{432g_3h_*^4 - \bar{g}_1} \gtrsim 60 \quad \rightarrow \quad 3\bar{g}_2h_*^2 \gtrsim 5\bar{g}_1 - 2052g_3h_*^4, \quad (51)$$

which means that if \bar{g}_2 is not too small then the classical trajectory can give enough e-foldings.

3.2 General cases with higher derivative terms

We can now extend our action by adding contractions of the Riemann tensor as

$$S = - \int d^4x \sqrt{-g} \left[\Lambda^4 g_0 + \Lambda^2 g_1 R + g_2 R^2 + g_{2a} R^{\mu\nu} R_{\mu\nu} + g_{2b} R^{\mu\nu\rho\sigma} R_{\mu\nu\rho\sigma} \right. \\ \left. + \Lambda^{-2} g_3 R^3 + \Lambda^{-2} g_{3a} R R^{\mu\nu} R_{\mu\nu} + \Lambda^{-2} g_{3b} R R^{\mu\nu\rho\sigma} R_{\mu\nu\rho\sigma} \right], \quad (52)$$

from which follows the relevant dynamical equation

$$\begin{aligned}
\bar{\mathcal{N}}(h, h', h'') &\equiv -\frac{2\Lambda^2}{H_0^6} \left(\frac{\delta S}{\delta g_{00}} \right)_{\text{FRW}} = 0 \\
&= [-\bar{g}_0 + 6\bar{g}_1 h^2 - (864g_3 + 216g_{3a} + 144g_{3b}) h^6] \\
&\quad + [-(216\bar{g}_2 + 72\bar{g}_{2a} + 72\bar{g}_{2b}) h^2 + (7776g_3 + 2160g_{3a} + 576g_{3b}) h^4] h' \\
&\quad + [(36\bar{g}_2 + 12\bar{g}_{2a} + 12\bar{g}_{2b}) + (3240g_3 + 1008g_{3a} - 216g_{3b}) h^2] h'^2 \\
&\quad - (432g_3 + 144g_{3a} + 144g_{3b}) h'^3 \\
&\quad + \{ [-(72\bar{g}_2 + 24\bar{g}_{2a} + 24\bar{g}_{2b}) h + (2592g_3 + 720g_{3a} + 288g_{3b}) h^3] \\
&\quad + (1296g_3 + 432g_{3a} + 144g_{3b}) h h' \} h'' = 0.
\end{aligned} \tag{53}$$

By comparing (38) and (53), one can see that the classical behavior of the quadratic terms in (52) can be reduced into that of the $f(R)$ case simply by replacing g_2 to

$$g_2 \rightarrow g_2 + \frac{g_{2a} + g_{2b}}{3}. \tag{54}$$

This fact can also be checked by considering the relations among the involved tensors and their special properties that appear in four dimensions. In four dimensions, the square of the Weyl tensor, $C_{\mu\nu\rho\sigma}$ is given as

$$C_{\mu\nu\rho\sigma}^2 = R_{\mu\nu\rho\sigma}^2 - 2R_{\mu\nu}^2 + \frac{1}{3}R^2. \tag{55}$$

The Euler scalar is given as

$$\chi_{\text{Euler}} = R_{\mu\nu\rho\sigma}^2 - 4R_{\mu\nu}^2 + R^2. \tag{56}$$

The variation of the general quadratic action can be written as

$$\begin{aligned}
&\delta \int d^4x \sqrt{-g} (g_2 R^2 + g_{2a} R_{\mu\nu}^2 + g_{2b} R_{\mu\nu\rho\sigma}^2) \\
&= \delta \int d^4x \sqrt{-g} g_2 R^2 + \delta \int d^4x \sqrt{-g} g_{2a} \left(\frac{1}{2} C_{\mu\nu\rho\sigma}^2 - \frac{1}{2} \chi_{\text{Euler}} + \frac{1}{3} R^2 \right) \\
&\quad + \delta \int d^4x \sqrt{-g} g_{2b} \left(2C_{\mu\nu\rho\sigma}^2 - 2\chi_{\text{Euler}} + \frac{1}{3} R^2 \right).
\end{aligned} \tag{57}$$

The variation of the C^2 term around a conformally flat metric like FRW is zero. The variation of Euler number vanishes identically (since it is a topological number of the manifold). Around the FRW background, thus, one has

$$\begin{aligned}
&\delta_{\text{FRW}} \int d^4x \sqrt{-g} (g_2 R^2 + g_{2a} R_{\mu\nu}^2 + g_{2b} R_{\mu\nu\rho\sigma}^2) \\
&= \left(g_2 + \frac{g_{2a}}{3} + \frac{g_{2b}}{3} \right) \delta_{\text{FRW}} \int d^4x \sqrt{-g} R^2,
\end{aligned} \tag{58}$$

confirming (54).

On the other hand, for the cubic order, we do not have the exact equivalence between (52) and $f(R)$ at the classical level. However, we can find a similar relation among g_3 's, which is crucial to determine the asymptotic behavior of the phase diagram, by comparing $\mathcal{C}(h)$'s. From (53), we read off $\mathcal{C}(h)$,

$$\mathcal{C}(h) = 864 \left(g_3 + \frac{g_{3a}}{4} + \frac{g_{3b}}{6} \right) h^6 - 6\bar{g}_1 h^2 + \bar{g}_0 = 0. \tag{59}$$

Then what we have discussed in the case of $f(R)$ is still valid in the general case with (52) by replacing g_3 to

$$g_3 \quad \rightarrow \quad g_3 + \frac{g_{3a}}{4} + \frac{g_{3b}}{6}. \quad (60)$$

Once the derivatives of the Ricci scalar, Ricci and Riemann tensor and their powers are added to the Lagrangian, the general behavior will change. However, this is beyond the scope of this work.

4 Quantum effects on the Hubble parameter

In this section, we study the quantum effects for the evolution of the Hubble parameter with (2). It is nontrivial to estimate its quantum fluctuations directly in the original frame, i.e. Jordan frame. One straightforward way is to derive them from the quantum fluctuations of the scalar field in Einstein frame, comparably easy to be calculated.

4.1 On the frame dependence of the quantum effects

We need to identify the relationship between the quantum fluctuations in Jordan and Einstein frame. From the conformal transformation between two frames,

$$g_{\mu\nu} \rightarrow \Omega(\phi)^2 g_{\mu\nu}, \quad (61)$$

with

$$\Omega(\phi) = e^{\sqrt{6}\phi/6\tilde{M}_p},$$

the Hubble parameter in Jordan frame can be estimated in Einstein frame,

$$H_J = e^{-\sqrt{6}\phi/6\tilde{M}_p} \left(H_E - \frac{\sqrt{6}}{6\tilde{M}_p} \dot{\phi} \right). \quad (62)$$

By taking the variation of (62), the quantum fluctuation in Jordan frame becomes

$$\Delta H_J = \left[\frac{\sqrt{6}}{6} \frac{H_J}{\tilde{M}_p} + \frac{\sqrt{2}f^{1/2}}{6} \frac{V^{1/2}}{\tilde{M}_p^2} (\sqrt{3\epsilon} - \epsilon + \eta) \right] \Delta\phi_q \quad (63)$$

$$\simeq \frac{\sqrt{6}}{6\tilde{M}_p} (H_J + \sqrt{\epsilon}\Omega H_E) \Delta\phi_q, \quad (64)$$

which holds under the slow-roll conditions,

$$H_E^2 \simeq \frac{V(\phi)}{3\tilde{M}_p^2} \quad \text{and} \quad \dot{\phi} \simeq -\frac{V'(\phi)}{3H_E}.$$

4.2 Classical drift vs. stochastic kick in Einstein frame

In Einstein frame, within the slow-roll approximation, the typical order of the classical drift of the scalar field ϕ during the Hubble time is estimated by

$$(\Delta\phi_c)^2 \equiv \left| \frac{\dot{\phi}}{H_E} \right|^2 \simeq 2\tilde{M}_p^2\epsilon. \quad (65)$$

On the other hand, from (196) in [11], a stochastic kick corresponding to the quantum fluctuation of ϕ during Hubble time is

$$(\Delta\phi_q)^2 \equiv \langle \delta\phi^2 \rangle = \frac{3H_E^4}{8\pi^2 m^2} \simeq \frac{1}{8\pi^2} \frac{H_E^2}{\eta}. \quad (66)$$

As the scalar field slowly rolls, both ϵ and η go to zero so that the classical drift gets smaller, but the quantum fluctuation gets bigger.

By comparing $(\Delta\phi_c)^2$ and $(\Delta\phi_q)^2$, one has H_0/Λ as an important parameter to identify the quantum dominant era. If the quantum fluctuation is dominant over the classical drift,

$$(\Delta\phi_c)^2 < (\Delta\phi_q)^2, \quad (67)$$

which implies

$$g_1 \left(\frac{\Lambda}{H_0} \right)^2 < \frac{1}{32\pi^2} \frac{1}{\epsilon\eta} \frac{1}{\Omega} \left(1 - 2\sqrt{\frac{\epsilon}{3}} \right) \approx 10^{-3} \times \frac{1}{\epsilon\eta}. \quad (68)$$

The parameter Λ/H_0 , the relative energy scale of inflation to the cutoff, leads us to judge how dominant the quantum effects would be. When g_1 is not too small, for instance, if Λ/H_0 is large enough to invalidate (68), then the quantum effects would be suppressed. In other words, the quantum effects would not be crucial if inflation occurs in a sufficiently low energy scale H_0 compared to the cutoff Λ . It is consistent with the naive intuition that inflation at the higher energy scale might have more chance to see quantum effects.

4.3 Quantum effects on the inflationary trajectories in Jordan frame

In order to understand how the quantum fluctuations affect the e-foldings, we evolve the inflationary trajectories in the (h, h') phase space by adding the quantum fluctuations in Jordan frame. Preliminarily, we find the classical trajectory with sufficiently large e-foldings (that is, passing near the h_* -point) for each $(\bar{g}_0, \bar{g}_1, \bar{g}_2, g_3)$ configuration. Since most of the classical or quantum contribution to the e-foldings comes from the h_* -point, and nonzero g_3 is simply related with \bar{g}_0 and \bar{g}_1 via (51), we focus only on the cases with $g_3 = 0$. We expect that the numerical results would give no differences between the cases with $g_3 = 0$ and with $g_3 \neq 0$. Using these trajectories, we evolve it again with the proper stochastic kicks which represent the quantum fluctuations.

The quantum correction Δh_q of h during the Hubble time can be estimated by substituting $\Delta\phi_q$ in (66),

$$\Delta h_q = \frac{\eta^{-1/2}}{12\sqrt{\pi}} \left[\frac{h}{\tilde{M}_p} + \sqrt{3} f^{1/2} \frac{V^{1/2}}{3\tilde{M}_p^2 H_0} (\sqrt{3\epsilon} - \epsilon + \eta) \right] \frac{V^{1/2}}{\tilde{M}_p}. \quad (69)$$

In the numerical calculation, we used a small time step $\Delta t \ll 1/H$ and calculated the the quantum correction of h during Δt , i.e. Δh_{rand} . Since the quantum fluctuation can be regarded as a random walk, and in a random walk the mean distance after N steps is \sqrt{N} times each step, the amplitude of Δh_{rand} is,

$$|\Delta h_{\text{rand}}| = |\Delta h_q| \times \sqrt{H\Delta t}. \quad (70)$$

Note that since $\bar{g}_0/\bar{g}_1 = 6$ and $g_3 = 0$, the quantum correction term depends on both \bar{g}_2/\bar{g}_1 and $\bar{g}_1(H_0/\Lambda)^2$, while the classical trajectory depends on \bar{g}_2/\bar{g}_1 only.

By incorporating the above quantum fluctuation, we iterated each $(\bar{g}_2/\bar{g}_1, \bar{g}_1(H_0/\Lambda)^2)$ configuration 500 times, and calculated the e-folding number distributions from

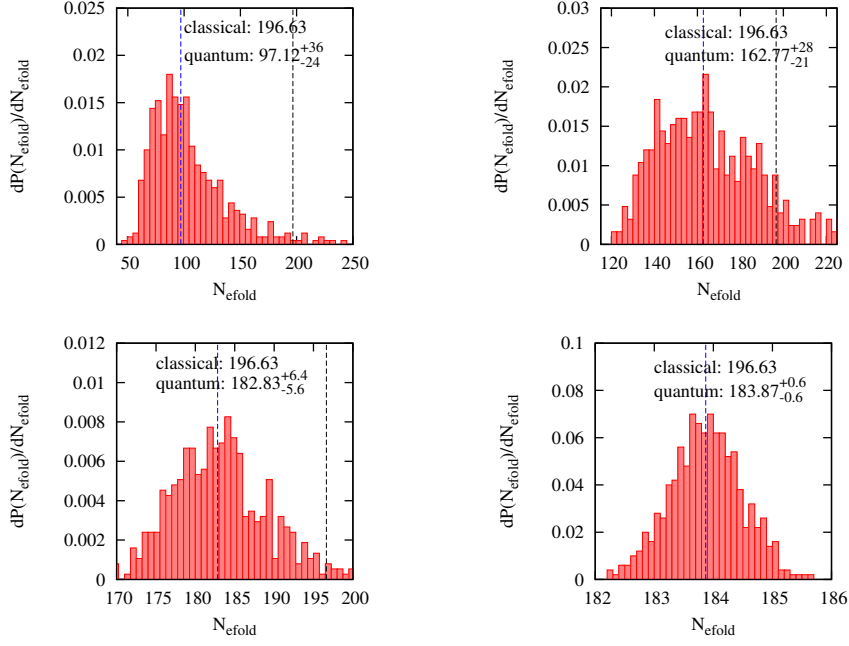


Figure 5: Probability distribution of e-foldings by considering quantum fluctuations, with $\bar{g}_2/\bar{g}_1 = 2$. Top-Left: $g_1 (\Lambda/H_0)^2 = 5 \times 10^1$; Top-Right: $g_1 (\Lambda/H_0)^2 = 5 \times 10^3$. Bottom-Left: $g_1 (\Lambda/H_0)^2 = 5 \times 10^5$; Bottom-Right: $g_1 (\Lambda/H_0)^2 = 5 \times 10^7$. Black line & “classical”: classical e-folding number; Blue line & “quantum”: medium value with 1σ -dispersion.

these 500 samples. Since the quantum fluctuation is much greater than the classical drift at $(h, h') = (1, 0)$ where most of the classical N_{efold} is generated, the medium value of N_{efold} can be different from the classical N_{efold} . The discrepancy between the classical N_{efold} and the medium value (and the width) of the probability distribution depends on $g_1 (\Lambda/H_0)^2$. Also, as shown in (70) both of them increase as $g_1 (\Lambda/H_0)^2$ decreases (see Figure 5).

Especially, if the quantum fluctuations become dominant, e.g. $g_1 (\Lambda/H_0)^2 \lesssim 10^1$, then the e-folding number significantly decreases, comparing with the classical e-folding number.

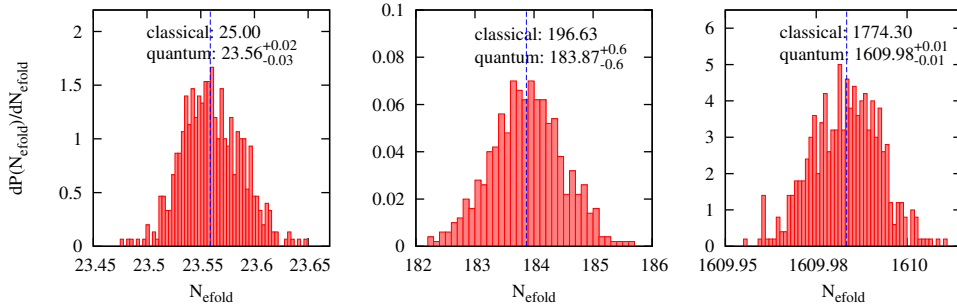


Figure 6: Probability distribution of e-folding number by considering quantum fluctuation, with $\bar{g}_1(H_0/\Lambda)^2 = 5 \times 10^7$. Left: $\bar{g}_2/\bar{g}_1 = 0.2$; Middle: $\bar{g}_2/\bar{g}_1 = 2$; Right: $\bar{g}_2/\bar{g}_1 = 20$. Black line & “classical”: classical e-folding number; Blue line & “quantum”: medium value with 1σ -dispersion.

On the other hand, if the quantum fluctuations become negligible, e.g. $g_1 (\Lambda/H_0)^2 \gtrsim$

10^2 , then the distribution of the e-foldings stays near the classical N_{efold} . As shown in (50), also, the entire distribution shifts toward the greater N_{efold} as \bar{g}_2/\bar{g}_1 increases (see Figure 6).

5 Discussion

In this paper, we discussed the possibility of inflation on higher derivative theories in the context of asymptotically safe gravity. Though the coupling constants are expected to be determined by the renormalization group flow, it gives nontrivial constraints on them that our universe has experienced the inflationary era. We could find the parametric relations between couplings by exploring successful inflationary trajectories on the phase diagrams in the bottom-up fashion. The asymptotic behaviors around the h_* -points, which are slow-roll points, are crucial for generating enough e-foldings and then escaping from the de Sitter state. The relative scale of inflation to the cutoff, i.e. H_0/Λ , is critical to control the quantum effects on the classical trajectory.

There are several topics for future works. It will be appealing to complete the map between higher derivative gravities and Einstein's gravity plus some scalar field theories. First, as we include general higher derivative terms, the types and the number of the fields will increase and the nontrivial couplings between such fields will be introduced [12]. Second, as in the standard Einstein side there are speculative themes such as eternal inflation and multiverse, it would be also intriguing to look for their counterparts in higher derivative gravities.

This work is only the first step to a realistic cosmological scenario from asymptotically safe gravity. It remains how to fill the whole cosmic history and to fit the observational constraints. We hope that higher derivative terms are initially dominant to produce the inflationary phase in the high energy scale, and then finally become negligible to allow Einstein's gravity. It is crucial to get a nontrivial evolution of the coupling constants. One may find possible ways by considering the dilatonic dependence on the couplings from string theory (e.g. [13]) or the energy scale dependence from the renormalization group flow [14, 15].

We need to study the cosmic perturbations during inflation and their evolution after inflation. It is a question whether we can have proper scalar, vector and tensor modes of the metric perturbations and make them evolve to produce the correct observations such as the power spectrum, the CMB and the production of gravitational waves. Cosmological perturbations, gravitational waves and cosmological vorticity have been studied within the quadratic theory [16]. Of course, it is crucial to look for a mechanism for reheating since the evolution of perturbations is dependent on the matter contents after reheating.

Acknowledgements

The authors thank to Bayram Tekin, Ewan Stewart, Hassan Firouzjahi, Wan-il Park, Tahsin Sisman, Dong-han Yeom, Alexei Starobinsky, Vincent Vennin, Chang Sub Shin and Dong-il Hwang. HZ thanks the hospitality of IPM where this work was progressed substantially. The authors are supported by Basic Science Research Program through the National Research Foundation of Korea(NRF) funded by the Ministry of Education, Science and Technology(2009-0077503). SEH is also supported by the National Research Foundation grant (2009-006814, 2007-0093860) funded by the Korean government. HZ is also supported by TÜBİTAK research fellowship programme for foreign citizens.

References

- [1] K. Stelle, Phys. Rev. D16, 953 (1977).
- [2] S. Weinberg, in *Understanding the Fundamental Constituents of Matter*, ed. A. Zichichi (Plenum Press, New York, 1977).
- [3] M. Niedermaier, Class. Quant. Grav. 24, R171 (2007), [gr-qc/0610018].
- [4] A. Codello and R. Percacci, Phys. Rev. Lett. 97, 221301 (2006), [hep-th/0607128]; A. Codello, R. Percacci and C. Rahmede, Annals Phys. 324, 414 (2009), [arXiv:0805.2909]; G. Narain and R. Percacci, Class. Quant. Grav. 27, 075001 (2010), [arXiv:0911.0386]; G. Narain and C. Rahmede, Class. Quant. Grav. 27, 075002 (2010), [arXiv:0911.0394]; D. Benedetti and P. F. Machado and F. Saueressig, Nucl. Phys. B824, 168 (2010), [arXiv:0902.4630].
- [5] S. Weinberg, Phys. Rev. D81, 083535 (2010), [arXiv:0911.3165].
- [6] A. Bonanno and M. Reuter, Phys. Rev. D65, 043508 (2002), [hep-th/0106133]; M. Hindmarsh, D. Litim and C. Rahmede JCAP 1107, 019 (2011), [arXiv:1101.5401]; Y.-F. Cai and D. A. Easson, [arXiv:1107.5815].
- [7] R. Brustein and G. Veneziano, Phys. Lett. B329, 429 (1994), [hep-th/9403060]; R. Brustein, M. Gasperini, M. Giovannini, V. F. Mukhanov and G. Veneziano, Phys. Rev. D51, 6744 (1995), [hep-th/9501066].
- [8] A. A. Starobinsky, Phys. Lett. B91, 99 (1980); M. B. Mijic, M. S. Morris and W.-M. Suen, Phys. Rev. D34, 2934 (1986).
- [9] S.-H. H. Tye and J. Xu, Phys. Rev. D82, 127302 (2010), [arXiv:1008.4787]
- [10] V. F. Mukhanov, H. A. Feldman and R. H. Brandenberger, Phys. Rept. 215, 203 (1992).
- [11] E. D. Stewart, Cosmology Lecture Note, http://cosmology.kaist.ac.kr/cos_grad/qfds_land.ps.
- [12] A. Hindawi, B. A. Ovrut and D. Waldram, Phys. Rev. D53, 5597 (1996), [hep-th/9509147].
- [13] A. L. Maroto and I. L. Shapiro, Phys. Lett. B414, 34 (1997), [hep-th/9706179];
- [14] M. Reuter and F. Saueressig, [arXiv:0708.1317]; A. Bonanno and M. Reuter, J. Phys. Conf. Ser. 140: 012008 (2008), [arXiv:0803.2546].
- [15] A. Bonanno, A. Contillo and R. Percacci, Class. Quant. Grav. 28, 145026 (2011), [arXiv:1006.0192].
- [16] H. Noh and J. Hwang, Phys. Rev. D59, 047501 (1999), [gr-qc/9811013]; Phys. Rev. D55, 5222 (1997), [gr-qc/9610059]; J. Hwang and H. Noh, Phys. Rev. D57, 2617 (1998), [gr-qc/9710035]